J Solid State Electrochem (2007) 11: 267–272
DOI 10.1007/s10008-006-0103-5

ORIGINAL PAPER

F. Hu · K. C. Chan · N. S. Qu

Effect of magnetic field on electrocodeposition behavior of Ni–SiC composites

Received: 30 August 2005 / Revised: 19 January 2006 / Accepted: 23 January 2006 / Published online: 28 February 2006

Abstract In this paper, an external magnetic field was applied in the electrodeposition of Ni–SiC composites, and its effects on surface morphology, SiC content, and crystal orientation were examined. It was found that the magnetic field modified the surface morphology and the orientation of the composites and significantly increased the SiC content. The phenomenon can be attributed to the change of charge transfer reactions and the mass transport process through the micromagnetohydrodynamic effect.

Keywords Ni–SiC composites · Magnetic field · Codeposition

Introduction

Over the past decades, external magnetic fields have presented various effects on the electrodeposition of metals and alloys [1–5]. Mohanta and Fahidy [6] observed that the cathodic limiting current of copper electrodeposition increased by 30% in an external magnetic field of 0.7 T. Without a magnetic field, the surface morphologies of iron grains were angular with a large size distribution, but they changed to roundish grains with smother surfaces in magnetic fields [7]. Nickel–iron deposits were also found to be modified by an imposed magnetic field, and resulted in a smoother deposit surface with a preferred orientation and uniform microstructure [8]. However, a magnetic field of 0.9 T in a two-electrode cell exerted only a limited effect on nickel grain orientation, although it produced grains with better-defined geometrical shapes [9]. It is generally agreed that the effect of a magnetic field is attributed to the magnetohydrodynamic effect due to the enhanced convection process induced by the Lorentz force. Based on experimental results, some empirical equations were developed to describe the relationship between mass transport limiting current, i_B, and magnetic field, **B**, in the electrodeposition of metals and alloys [10, 11]. Aogaki et al. also showed that i_B varied with $\mathbf{B}^{1/3}$, and an empirical equation describing the effects of a strong magnetic field on the mass transport limiting current for electrodeposition on disk platinum electrodes using chronoamperometry was developed by Legeai et al. [11]. An in-depth analysis to understand the detailed mechanisms of the effect of magnetic fields has yet to be done.

Composite materials have been widely investigated and successfully applied in the automotive and aerospace industry as a result of their improved mechanical and tribological properties. The distribution and volume fraction of second-phase particles on the deposit surface play an important role on the properties of composites [12]. There is a significant amount of work to study the electrocodeposition of composites, but relatively less work has been done to examine the effect of magnetic fields, although it is known that magnetic fields affect the codeposition process [10]. With the aim to improve the properties of electrocomposites by controlling their microstructure, the effect of magnetic fields on surface morphology, crystal orientation, and the SiC content of the Ni–SiC composites will be examined in this paper for the first time.

Experimental

In this paper, a two-electrode glass cell for nickel deposition with an electrolyte volume of 100 ml was used. A stainless steel cathode mandrel with dimensions of 30 × 30 × 1 mm, and a stainless steel anode electrode, which was unattractable to the magnetic field, were used. The schematic diagram of the magneto-electrolysis setup is shown in Fig. 1. The composition of the bath solution was nickel sulfamate 330 g/l, nickel chloride 15 g/l, boric acid 30 g/l, and sodium dodecyl sulfate 1 g/l. An amount of 40 g/l of SiC particles (β SiC), with a diameter of about 100 nm, was

F. Hu · K. C. Chan (✉) · N. S. Qu
Advanced Manufacturing Technology Research Center,
Department of Industrial and Systems Engineering,
The Hong Kong Polytechnic University,
Hung Hom, Hong Kong
e-mail: mfkcchan@polyu.edu.hk
Tel.: +852-2-7664981
Fax: +852-2-3625267

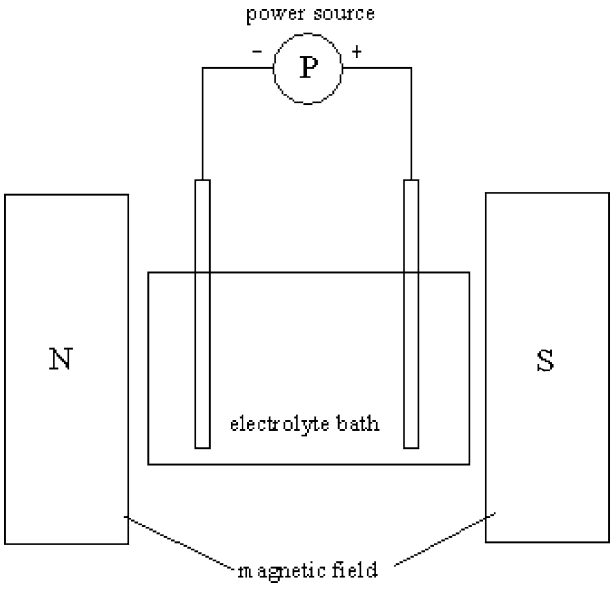

Fig. 1 The schematic diagram of the electrodeposition setup

added. The electrolyte was agitated by a mechanical stirrer, temperature was kept at 50°C, and the initial pH of the electrolyte was 4.2, which is a typical value used in electroplating.

Electrochemical impedance spectra (EIS) of the deposition system were acquired in the frequency range of 30 kHz to 5 mHz, with a 10-mV amplitude sine wave generated by a frequency response analyzer, and a thin layer of composite was deposited before each set of measurements. A three-electrode setup was used in the electrochemical measurements, and the reference electrode was an Ag/AgCl electrode with a KCl-saturated aqueous solution. The data obtained were corrected for ohmic drop. After electroplating, SEM (Leica Steroscan 440) and an energy dispersive X-ray were used to study the surface morphology and composition of the Ni–SiC composite. The preferred crystal orientation was measured by X-ray diffraction (XRD) using the Cu–Kα line (X'Pert, Philips, 40 kV, 30 mA). To evaluate quantitatively the preferred orientation, an orientation index was used and the calculation method was based on that of Matsushima et al. [13].

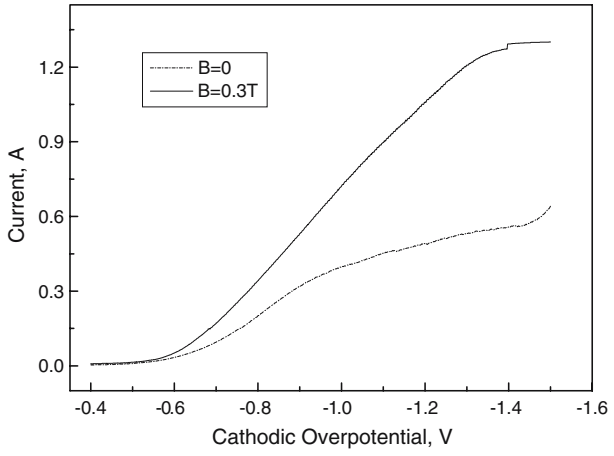

Fig. 2 Current–potential curves for Ni–SiC electrodeposition with and without a magnetic field vs reference electrode Ag/AgCl

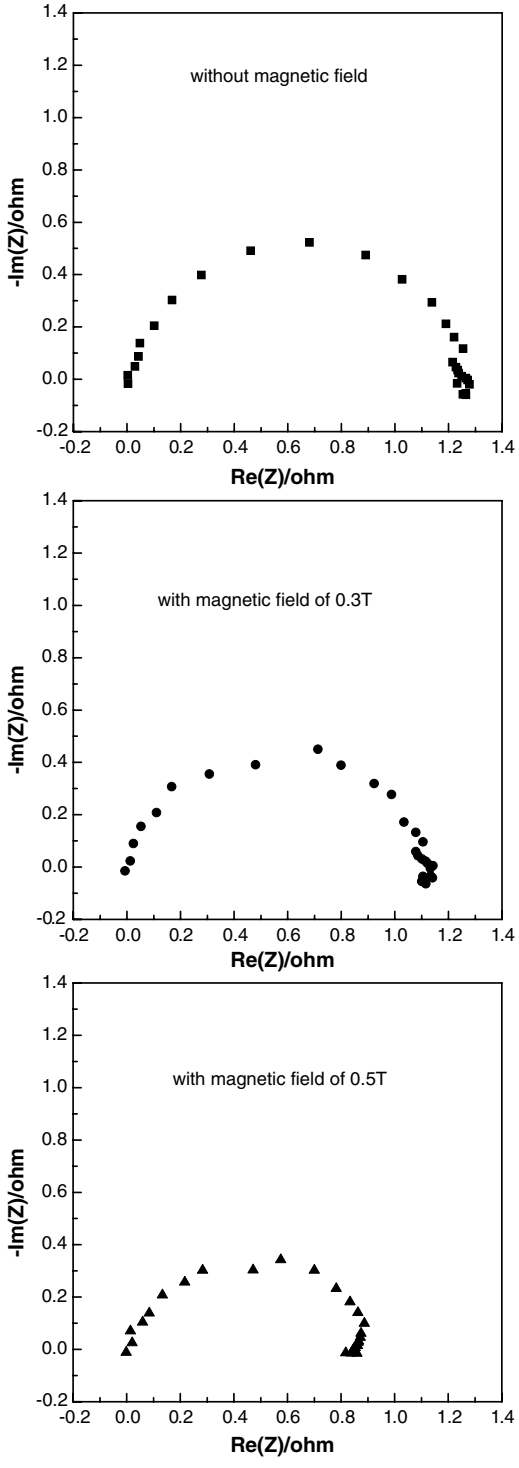

Fig. 3 Nyquist plots of Ni–SiC electrodeposition system at the cathodic potential of −700 mV vs reference electrode Ag/AgCl

Table 1 The charge transfer resistances and double layer capacitances obtained for the Ni–SiC electrodeposition system with and without magnetic fields

B (T)	$-\eta$ (mV)	R_{ct} (Ω)	C_{dl} (μF)	$R_{ct}I$ (V)	Chi squared value
0	600	1.782	373.6	0.0597	0.0004954
	700	1.555	395.8	0.1477	0.001229
	800	0.6273	661.3	0.1261	0.0026
0.3	600	1.246	382.4	0.0645	0.0009928
	700	0.8644	540.1	0.1456	0.001757
	800	0.3406	716.4	0.1165	0.00958

Results and discussion

Linear sweep voltammetry

The voltammogram of the Ni–SiC electrodeposition system with and without a magnetic field is shown in Fig. 2. Without a magnetic field, the polarization curve has three typical electrochemical regions: the activation region at low overpotentials, the mass transfer region (characterized by the current plateau) and the third region characterizing hydrogen evolution (with the cathodic potential higher than −1.4 V). With a magnetic field of 0.3 T, a rapid increase in current is observed when the cathodic potential is less than −0.6 V vs Ag/AgCl, and no current plateau is observed. Similar results were also reported in the deposition of Ni–Fe alloy at magnetic fields ranging from 0 to 0.9 T [8], and in copper deposition from 0 to 0.178 T [14].

This phenomenon may be attributed to the micromagnetohydrodynamic (micro-MHD) effect [15, 16], which enhances the convection process (as well as the motion of ions and particles) in the electrolyte, leading to an increase in Faradic current and limiting current. A higher limiting current density is shown to result in an increase in current efficiency and a more uniform current distribution, which will improve the physical and mechanical properties of the deposits [8, 17–20]. It is generally known that the mass transport process is related to the thickness of the diffusion layer, δ, and its value is determined by the limiting current density through the equation: $j = \frac{nFDc}{\delta}$, where n, F, D, and c are constant [21]. A higher limiting current obviously reduces the thickness of the diffusion layer, and Danilyuk et al. [14] even believed that the diffusion layer is essentially reconstructed due to the MHD effects.

Impedance analysis

The electrodeposition of metals is an adsorption and crystallization process. With the change of mass transport process and limiting current density, the reduction reactions are expected to be more complicated. To understand the process, the EIS were examined. Figure 3 gives the Nyquist plots of EIS curves with and without a magnetic field at the cathodic potential of −700 mV, and they are corrected for the solution resistance. The capacitive loop under the magnetic field of 0 T is a half circle. While the capacitive loop for the magnetic field of 0.3 T is depressed, the capacitive loop for 0.5 T is more distorted. The shapes and characteristics of the impedance spectra which are related to the cathodic reactions are shown to be affected by the magnetic field. In fact, in a copper electrodeposition system, the transformation from one capacitive loop to two indistinguishable capacitive loops was also observed [17], and the author proposes a pseudocapacitance to illustrate the depressed capacitive loop.

Based on the equivalent circuit of Chopart et al. [17], the EIS curves at different cathodic overpotentials ranging from −600 mV to −1,050 mV were best fitted by the software ZsimpWin to obtain the charge transfer resistances and the double layer capacitances. The results are shown in Table 1. It is worth mentioning that the time constant of the first loop is higher than that of the second one, and the first charge transfer reaction is believed to be the determining step in the electrocodeposition process under a magnetic field. Table 1 shows that the charge transfer resistance is changed by the magnetic field. Similar phenomena were observed by other researchers. Devos et al. [19] found a decrease of R_{ct} from 7.6 Ω at 0.15 T to 4.0 Ω at 0.9 T in the zinc electrodeposition system. For nickel electrodeposition, the amplitude of the capacitive loop also increased with an increasing magnetic field [22]. Msellak et al. [8] also observed that the amplitude increased when the magnetic field increased from 33 Ω at 0 T to 39 Ω at 0.9 T in a Ni–Fe alloy codeposition. It is also

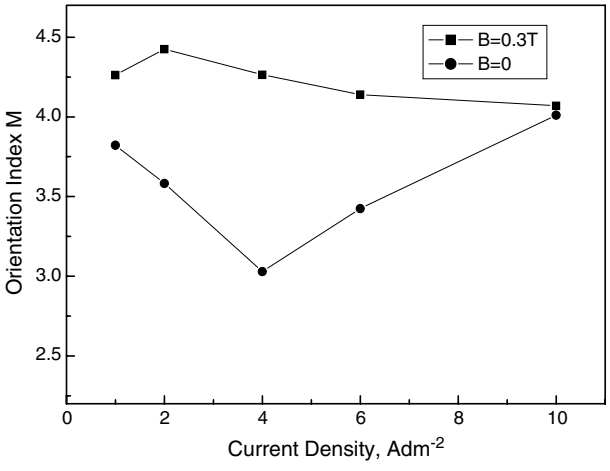

Fig. 4 Dependence of (200) orientation index on current density in Ni–SiC electrodeposition

worth pointing out that the product of the charge-transfer resistance and the electrolysis current is approximately constant in the whole overpotential range, which illustrates that the magnetic field does not affect the charge transfer coefficient. Similar phenomena were reported by other researchers [13, 19, 22]. However, the data obtained from these studies are far from sufficient to explain and understand the effect of magnetic fields on charge transfer kinetics, and more work has yet to be done.

The presence of magnetic fields also changes the features of the inner cathodic surface, which can be estimated by the double-layer thickness between the metal and electrolyte. In a parallel plate, the thickness of the double layer, x_d, can be expressed by the equation [18]: $x_d = \frac{\varepsilon\varepsilon_0 A}{C_{dl}}$, where ε is the relative permittivity of the medium and ε_0 is the permittivity of free space. As a larger value of C_{dl} is obtained with an external magnetic field, as shown in Table 1, the thickness of the double layer will be slightly reduced according to the above equation.

Crystal orientation

XRD patterns were obtained for the Ni–SiC composites, and under all the testing conditions, the relative intensity of the (200) orientation is the largest. Figure 4 summarizes the intensity of the (200) orientation at different current densities without and with a magnetic field of 0.3 T. It is clear that the intensity of the (200) orientation with the magnetic field is significantly higher than those without magnetic fields. Such an increase can be attributed to the micro-MHD effect. The electrocrystallization of nickel is known as a highly inhibited process and the (200) texture mode of crystal growth is inhibited by chemical species, such as nickel hydroxide and hydrogen ions [23]. As

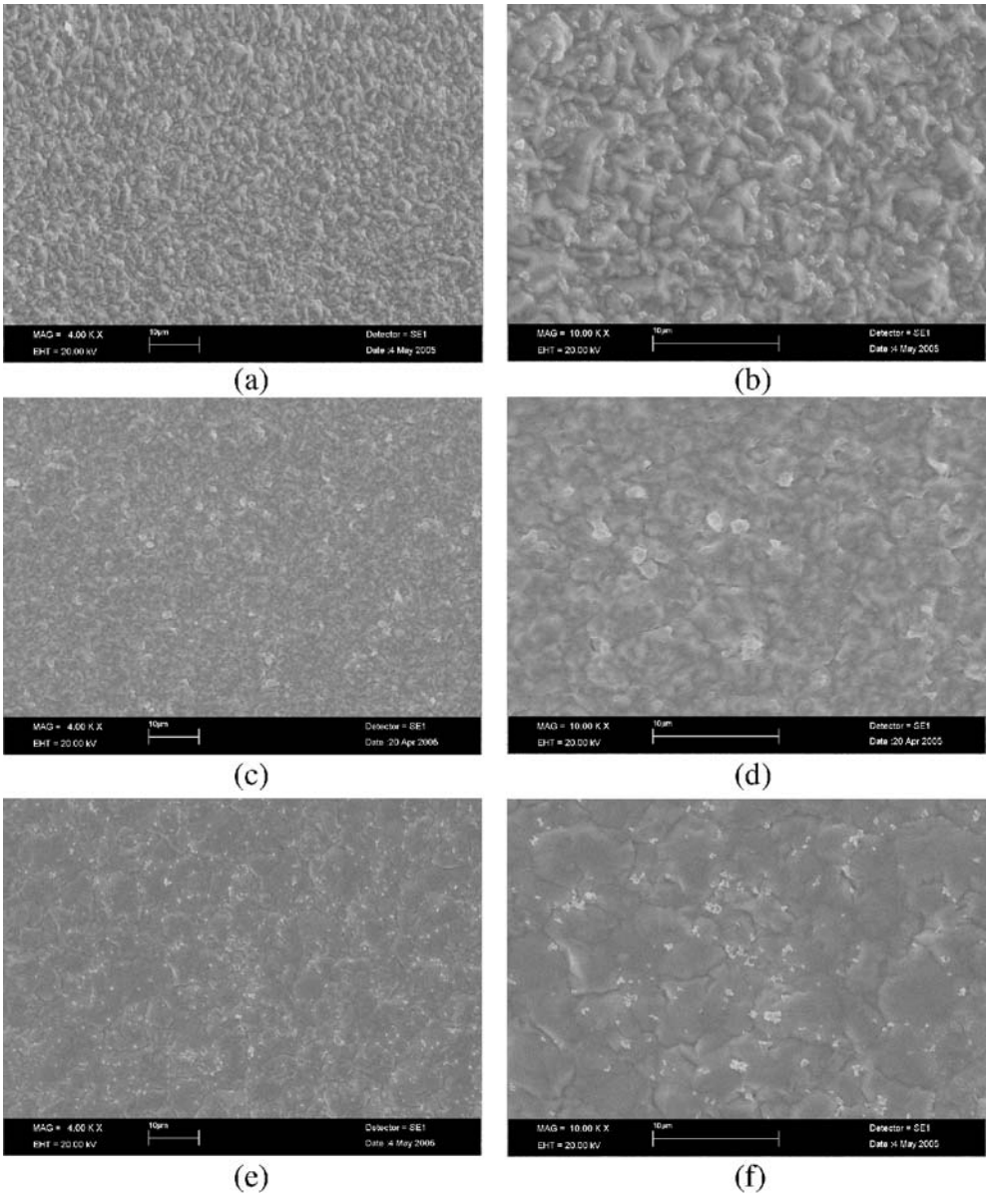

Fig. 5 SEM micrographs of Ni–SiC deposits obtained in the two-electrode cell with a 100-ml sulfamate bath and without an external magnetic field. Current density: 1 (**a**, **b**), 4 (**c**, **d**), and 10 Adm^{-2} (**e**, **f**). Magnification: ×4,000 (**a**, **c**, **e**); ×10,000 (**b**, **d**, **f**)

discussed above, the magnetic field of 0.3 T reduces the thickness of the diffusion layer, which will result in the enhancement of hydrogen evolution [7], and the concentration of hydrogen ions close to the cathode surface is consequently reduced. The electrocrystallization process becomes less inhibited, and it favors the formation of (200) grains. Without a magnetic field, a minimum intensity is observed at a current density of 4 Adm^{-2}. The change of the (200) orientation index is attributed to the change in the amount of inhibiting chemical species. As the intensity of the (200) orientation decreases with increasing current density when the current density is below 4 Adm^{-2}, the amount of inhibiting species should increase with the increasing current density. However, it is expected that the amount will decrease when the current density is above 4 Adm^{-2}, as the intensity of the (200) orientation increases. It is interesting to note that, at the current density of 10 Adm^{-2}, about the same intensity is obtained with or without a magnetic field. It is considered that such a high current density induces a very significant hydrogen evolution process, and the influence of magnetic field on the process becomes secondary.

Morphology and composition

Figure 5 shows the surface morphologies of the Ni–SiC composites obtained at current densities of 1, 4, and 10 Adm^{-2} without a magnetic field. It is found that the surface morphologies are influenced by the current density as the values of surface roughness decrease with increasing current density. Pyramidal grains and a rough composite surface are observed at a current density of 1 Adm^{-2}, and a flat surface with roundish grains is observed at a current density of 10 Adm^{-2}. The average SiC content of the composites is about 1.22 at.%.

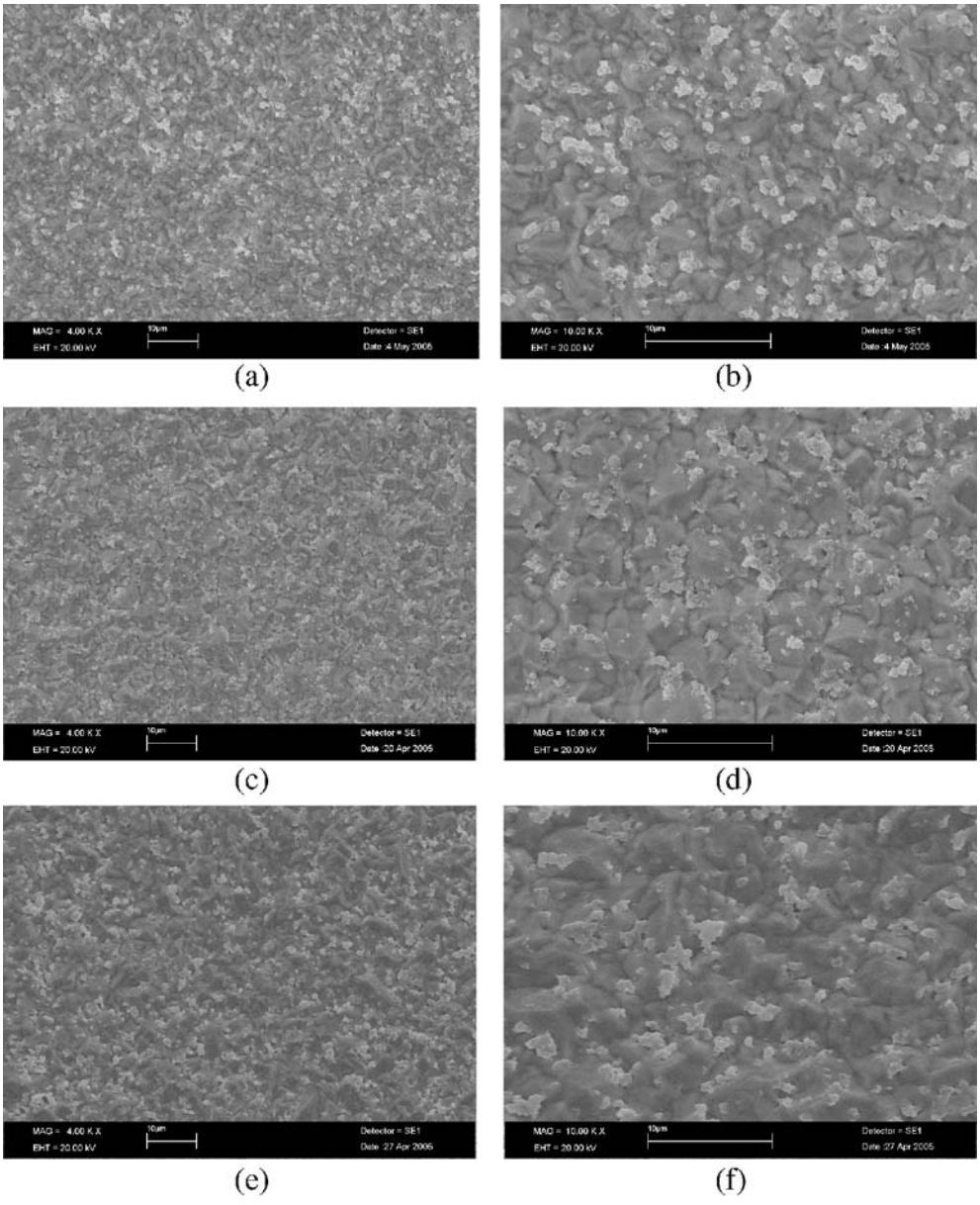

Fig. 6 SEM micrographs of Ni–SiC deposits obtained in the two-electrode cell with a 100-ml sulfamate bath and with a magnetic field of 0.3 T. Current density: 1 (**a**, **b**), 4 (**c**, **d**), and 10 Adm^{-2} (**e**, **f**). Magnification: ×4,000 (**a**, **c**, **e**); ×10,000 (**b**, **d**, **f**)

With the aid of an external magnetic field of 0.3 T, the surface morphologies obtained under current densities of 1, 4, and 10 Adm^{-2} are shown in Fig. 6. The nickel matrix grains are modified by the magnetic field (as compared to the morphologies as shown in Fig. 5). This is probably due to the change of reduction passage of nickel ions. The Lorentz force drives the ions moving around the magnetic flux. Without a magnetic field, the ions are transferred from the anode to the cathode, and the normal direction of ion transfer is toward the cathode mandrel. Moreover, the incorporation of SiC particles is greatly improved under the existence of a magnetic field; the particle codeposition process may also interfere with the electrocrystallization of nickel and modify the surface morphology of Ni–SiC composites.

Compared to the composites synthesized without a magnetic field, the amounts of SiC particles in the composites are greatly enhanced to an average content of 3.26 at.%. It is known that SiC particles do not exist solely in the electrolyte solution. These particles are adsorbed by nickel ions, transported to the cathode, and deposited with nickel ion reduction [24]. The SiC particles are actually charged particles and influenced by applied fields. The increase in SiC content might be explained by the micro-MHD effect in terms of the local Lorentz force and the charge transfer process. The local Lorentz force enhances the convection process, which is favorable for maintaining the suspension of particles and for transporting them to the electrode surface. It will offer a higher chance for the SiC particles to contact with the cathode electrode and to be embedded in the deposit. On the other hand, the micro-MHD effect increases the limiting current, as well as the rate of charge transfer. The codeposition phenomenon is explained as a competition process between particle adhesion and removing [25], and the codeposition mechanism is also explained as a charge transfer controlled process [26]. In the present work, a higher charge transfer rate is obtained under the same current density. As suggested by Guglielmi's model, this will result in a more rapid process for the incorporation of particles in the composite [27]. The investigation of magneto-electrolysis is of significant industrial and academic value. It may open up a novel method of modifying the microstructure, in particular the particle content, by controlling the magnetic fields with no need to adjust additives, bath composition, and volume percentage of particles throughout the process. The findings of this paper help us to better understand the magnetohydrodynamic effect in the electrodeposition of composites.

Conclusion

The effects of a magnetic field of 0.3 T on the electrodeposition behavior and microstructure of Ni–SiC composites were studied in a sulfamate bath. Based on the impedance analysis, the micro-MHD effect is shown to be significant in improving the mass transport process and accelerating the charge transfer rate. It was found that the surface morphology and grain orientation of the composites were modified by the magnetic field. A significant increase of SiC content is also observed in the composites with the magnetic field, and it is attributed to the improvements of the convection and charge transfer process. This study presents a novel alternative method of modifying the microstructures of the composites and enhancing the content of embedding particles.

Acknowledgements The work described in this paper was supported by a grant from the Research Grant Council of The Hong Kong Special Administration (project number Poly-U5185/01E). Support from The Hong Kong Polytechnic University is also acknowledged.

References

1. Chiba A, Ogawa T, Yamashita T (1988) Surf Coat Technol 34:455
2. Chiba A, Kitamura K, Ogawa T (1986) Surf Coat Technol 27:83
3. Nikolic ND, Wang H, Cheng H, Guerrero CA, Garcia N (2004) J Magn Magn Mater 2436:272
4. Li XP, Zhao ZJ, Seet HL, Heng WM, Oh TB, Lee JY (2004) Electrochem Solid State Lett 7(1):C1
5. Gu ZH, Fahidy TZ (2000) J Phys D Appl Phys 33:L113
6. Mohanta S, Fahidy TZ (1972) Can J Chem Eng 50:248
7. Matsushima H, Nohira T, Mogi I, Ito Y (2004) Surf Coat Technol 179:245
8. Msellak K, Chopart JP, Jbara O, Aaboubi O, Amblard J (2004) J Magn Magn Mater 281:295
9. Brillas E, Rambla J, Casado J (1999) J Appl Electrochem 29:1367
10. Tacken RA, Janssen LJJ (1995) J Appl Electrochem 25:1
11. Legeai S, Chatelut M, Vittori O, Chopart JP, Aaboubi O (2004) Electrochim Acta 50:51
12. Hu F, Chan KC (2004) Appl Surf Sci 233:163
13. Matsushima H, Nohira T, Ito Y (2004) J Solid State Electrochem 8:195
14. Daniyuk AL, Kurmashev VI, Matyushkov AL (1990) Thin Solid Films 189:247
15. Shinohara K, Aogaki R (1999) Electrochemistry 67:126
16. Matsushima H, Nohira T, Ito Y (2004) Electrochem Solid State Lett 7:C81
17. Chopart JP, Douglade J, Fricoteaux P, Olivier A (1991) Electrochim Acta 36:459
18. Hinds G, Spada FE, Coey JMD, Ni Mhiochain TR, Lyons MEG (2001) J Phys Chem B 105:9487
19. Devos O, Aaboubi O, Chopart JP, Merienne E, Olivier A, Gabrielli C, Tribollet B (1999) J Phys Chem B 103:496
20. Aaboubi O, Amblard J, Chopart JP, Olivier A (2004) J Electrochem Soc 151(2):C112
21. O'reilly C, Hinds G, Coey JMD (2001) J Electrochem Soc 148 (10):C674
22. Devos O, Azboubi O, Chopart JP, Meienne E, Olivier A, Amblard J (1998) J Electrochem Soc 145:4135
23. Chan KC, Qu NS, Zhu D (1998) Surf Coat Technol 99:69
24. Yeh SY, Wan CC (1994) J Appl Electrochem 24:993
25. Fransaer J, Celis JP, Roos JR (1992) J Electrochem Soc 139 (2):413
26. Shretha NK, Miwa I, Saji T (2001) J Electrochem Soc 148(2):C106
27. Guglielmi N (1972) J Electrochem Soc 1009